Effect of Hydrophobic Residue Substitutions with Glutamine on Ca^{2+} Binding and Exchange with the N-Domain of Troponin C†

Svetlana B. Tikunova,‡,§ Jack A. Rall,§ and Jonathan P. Davis*,§

Department of Molecular and Cellular Biochemistry and Department of Physiology and Cell Biology, The Ohio State University, Columbus, Ohio 43210

Received September 5, 2001; Revised Manuscript Received April 2, 2002

ABSTRACT: Troponin C (TnC) is an EF-hand Ca^{2+} binding protein that regulates skeletal muscle contraction. The mechanisms that control the Ca^{2+} binding properties of TnC and other EF-hand proteins are not completely understood. We individually substituted 27 Phe, Ile, Leu, Val, and Met residues with polar Gln to examine the role of hydrophobic residues in Ca^{2+} binding and exchange with the N-domain of a fluorescent TnC^{F29W}. The global N-terminal Ca^{2+} affinities of the TnC^{F29W} mutants varied ∼2340-fold, while Ca^{2+} association and dissociation rates varied less than 70-fold and more than 45-fold, respectively. Greater than 2-fold increases in Ca^{2+} affinities were obtained primarily by slowing of Ca^{2+} dissociation rates, while greater than 2-fold decreases in Ca^{2+} affinities were obtained by slowing of Ca^{2+} association rates and speeding of Ca^{2+} dissociation rates. No correlation was found between the Ca^{2+} binding properties of the TnC^{F29W} mutants and the solvent accessibility of the hydrophobic amino acids in the apo state, Ca^{2+} bound state, or the difference between the two states. However, the effects of these hydrophobic mutations on Ca^{2+} binding were contextual possibly because of side chain interactions within the apo and Ca^{2+} bound states of the N-domain. These results demonstrate that a single hydrophobic residue, which does not directly ligate Ca^{2+}, can play a crucial role in controlling Ca^{2+} binding and exchange within a coupled and functional EF-hand system.

Troponin C (TnC)[1] is a Ca^{2+} binding protein involved in the regulation of striated muscle contraction and relaxation as a part of the Tn complex (for review, see refs *1*−*3*). Skeletal muscle TnC consists of N- and C-terminal globular domains connected by a 31-residue central α-helix (for review, see refs *4*, *5*). Each globular domain binds two Ca^{2+} ions through a pair of EF-hand helix−loop−helix Ca^{2+} binding motifs. The two loops of the adjacent EF-hands interact with each other through a short antiparallel *β*-sheet. The EF-hands are numbered I−IV, and the helices flanking the loops are designated A−H. The N-domain of TnC has an additional 14-residue α-helix (N-helix), which is absent in a closely related EF-hand Ca^{2+} binding protein, calmodulin (CaM). The two N-terminal EF-hands selectively bind Ca^{2+}, while the two C-terminal EF-hands have a higher Ca^{2+} affinity and also bind Mg^{2+} (*6*). The C-terminal sites of TnC in skeletal muscle are thought to be always occupied by either Ca^{2+} or Mg^{2+}. Therefore, it is believed that the C-domain of TnC plays a structural role by anchoring TnC into the Tn complex, while the N-domain directly regulates muscle contraction and relaxation through Ca^{2+} binding and release.

Skeletal muscle contraction is initiated when cytoplasmic [Ca^{2+}] rises, which allows binding of Ca^{2+} to the N-terminal EF-hands of TnC. Upon Ca^{2+} binding, the N-domain of TnC undergoes a large tertiary conformational change in which helices B and C (BC unit) move away as a unit from helices N, A, and D (NAD unit). This leads to the exposure of hydrophobic residues at the protein surface, allowing the quaternary interaction of the N-domain of TnC with the C-domain of TnI, which initiates the cascade of events that leads to muscle contraction. As cytoplasmic [Ca^{2+}] lowers, Ca^{2+} dissociates from the N-domain of TnC, burying the hydrophobic residues and preventing the interaction of the N-domain with the C-domain of TnI, and subsequently the muscle relaxes.

EF-hand Ca^{2+} binding proteins exhibit a wide variety of Ca^{2+} binding affinities (∼10^6-fold variation) and dissociation rates (>10^4-fold variation) (for review, see refs *7*−*11*). Factors that control Ca^{2+} binding and exchange are quite complex and involve residues within and outside of the Ca^{2+} binding loops (*12*, *13*). We have recently examined the role of acidic residues in chelating positions in Ca^{2+} binding and exchange with the N-terminal EF-hands of CaM. By varying the number and location of acidic residues in chelating positions (excluding the relatively invariant $+x$ and $-z$

† This research was funded, in part, by NIH Grant DK33727 to Dr. Ruth A. Altschuld (Department of Molecular and Cellular Biochemistry, The Ohio State University), NIH Grant AR20792 to Dr. Jack A. Rall, and an award from the American Heart Association, Ohio Valley Affiliate, to Dr. Jonathan P. Davis.

* To whom correspondence should be addressed. Address: Department of Physiology and Cell Biology, The Ohio State University, 304 Hamilton Hall, 1645 Neil Avenue, Columbus, OH 43210. Phone: 614-292-6137. Fax: 614-292-4888. E-mail: davis.812@osu.edu.

‡ Department of Molecular and Cellular Biochemistry.

§ Department of Physiology and Cell Biology.

[1] Abbreviations: Tn, troponin; TnC, chicken skeletal troponin C.; TnC^{F29W}, TnC mutant with the Phe 29 → Trp mutation; CaM, calmodulin; MOPS, 3-(*N*-morpholino)propanesulfonic acid; EGTA, ethylene glycol bis(*β*-aminoethyl ether)-*N*,*N*,*N*′,*N*′-tetraacetic acid; IPTG, isopropylthio-*β*-D-galactopyranoside; Quin-2, 2-((bis(carboxymethyl)-amino)-5-methylphenoxy)methyl)-6-methoxy-8-(bis(carboxymethyl)-amino)quionline.

10.1021/bi011763h CCC: $22.00
Published on Web 05/02/2002

Table 1: Summary of Ca^{2+} Binding Properties for TnC^{F29W} and Its Mutants[a]

mutant protein	K_d (μM)	Hill coeff	k_{off} (Trp) (s^{-1})	k_{off} (Quin) (s^{-1})	$k_{on} \times 10^8$ (Trp) ($M^{-1}\ s^{-1}$)	SA apo (%)	SA Ca^{2+} (%)	SA (Ca^{2+} − apo) (%)
TnC^{F29W}	3.2 ± 0.2	1.9 ± 0.2	340 ± 22	346 ± 11	1.1	23 ± 5	30 ± 5	7
$M3QTnC^{F29W}$	3.0 ± 0.3	2.3 ± 0.2	380 ± 22	382 ± 6	1.3	22 ± 12	66 ± 15	44
$F13QTnC^{F29W}$	2.5 ± 0.3	1.8 ± 0.2	272 ± 8	296 ± 14	1.1	44 ± 7	57 ± 18	13
$L14QTnC^{F29W}$	5.9 ± 0.4	2.2 ± 0.2	341 ± 17	355 ± 9	0.6	11 ± 8	3 ± 5	−8
$M18QTnC^{F29W}$	2.55 ± 0.05	1.89 ± 0.04	273 ± 13	279 ± 4	1.1	29 ± 7	41 ± 8	12
$I19QTnC^{F29W}$	4.4 ± 0.9	2.2 ± 0.4	447 ± 9	445 ± 5	1.1	21 ± 7	15 ± 5	−6
$F22QTnC^{F29W}$	0.99 ± 0.03	2.05 ± 0.02	95 ± 1	96 ± 1	1.0	3 ± 2	12 ± 5	9
$F26QTnC^{F29W}$	395 ± 30	1.32 ± 0.09	>1000	>1000	>0.03	1 ± 1	5 ± 2	4
$M28QTnC^{F29W}$	3.8 ± 0.3	1.6 ± 0.2	362 ± 20	326 ± 3	1	63 ± 5	56 ± 11	−7
$I37QTnC^{F29W}$	78 ± 8	1.01 ± 0.03	623 ± 34	345 ± 22	0.08	1 ± 1	2 ± 1	1
$L42QTnC^{F29W}$	6 ± 1	1.2 ± 0.1	246 ± 10	230 ± 18	0.4	0 ± 0	6 ± 2	6
$V45QTnC^{F29W}$	0.17 ± 0.02	1.8 ± 0.1	25.3 ± 0.2	24 ± 1	1.5	0 ± 0	8 ± 5	8
$M46QTnC^{F29W}$	0.88 ± 0.06	1.7 ± 0.1	93 ± 4	90 ± 2	1.1	0 ± 0	23 ± 5	23
$M48QTnC^{F29W}$	3.2 ± 0.4	1.8 ± 0.2	324 ± 16	331 ± 9	1.0	59 ± 7	68 ± 10	9
$L49QTnC^{F29W}$	0.169 ± 0.002	1.52 ± 0.02	34.7 ± 0.4	34.2 ± 0.8	2.1	19 ± 4	86 ± 9	67
$L58QTnC^{F29W}$	4.0 ± 0.4	2.2 ± 0.2	687 ± 12	689 ± 18	1.7	12 ± 5	2 ± 2	−10
$I61QTnC^{F29W}$	2.57 ± 0.05	1.96 ± 0.08	516 ± 23	518 ± 19	2.0	10 ± 5	46 ± 6	36
$I62QTnC^{F29W}$	37 ± 4	1.18 ± 0.03	1137 ± 150	>1000	0.3	16 ± 4	1 ± 1	−15
$V65QTnC^{F29W}$	8 ± 1	1.9 ± 0.2	298 ± 8	298 ± 1	0.4	5 ± 5	12 ± 5	7
$I73QTnC^{F29W}$	22.8 ± 0.9	1.82 ± 0.04	413 ± 25	402 ± 9	0.2	0 ± 1	4 ± 3	4
$F75QTnC^{F29W}$	4.4 ± 0.2	1.8 ± 0.1	378 ± 11	410 ± 12	0.9	11 ± 4	22 ± 5	11
$F78QTnC^{F29W}$	27 ± 4	1.7 ± 0.1	377 ± 6	334 ± 15	0.1	0 ± 0	15 ± 7	15
$L79QTnC^{F29W}$	9.8 ± 0.1	1.47 ± 0.09	403 ± 15	402 ± 19	0.4	2 ± 1	3 ± 2	1
$V80QTnC^{F29W}$	22 ± 4	1.53 ± 0.07	829 ± 69	690 ± 30	0.4	3 ± 3	11 ± 6	8
$M81QTnC^{F29W}$	19 ± 4	1.74 ± 0.05	723 ± 30	791 ± 41	0.4	4 ± 3	21 ± 5	17
$M82QTnC^{F29W}$	0.69 ± 0.05	1.91 ± 0.03	76 ± 6	73 ± 1	1.1	0 ± 1	29 ± 8	29
$V83QTnC^{F29W}$	3.7 ± 0.5	2.2 ± 0.2	518 ± 22	522 ± 8	1.4	2 ± 2	14 ± 9	12
$M86QTnC^{F29W}$	2.6 ± 0.3	1.7 ± 0.3	372 ± 7	377 ± 5	1.4	17 ± 5	42 ± 16	25

[a] Solvent accessibility (SA) for hydrophobic amino acids is represented as a mean ± SD. Each K_d, Hill coefficient, and k_{off} represents a mean ± SD of three to five experiments, and each is fit separately.

chelating residues), we were able to obtain CaM mutants with only 22-fold variation in their Ca^{2+} affinities (*14*). These studies suggested that other factors, such as hydrophobicity of the helices and nonchelating loop residues, are also involved in controlling Ca^{2+} binding and exchange. For example, Kragelund et al. (*15*) demonstrated that mutation of hydrophobic core residues strongly influenced the Ca^{2+} binding properties of calbindin D_{9k}. We were especially interested in understanding how hydrophobic amino acids affect Ca^{2+} binding and exchange with the N-domain of TnC.

Previously, Pearlstone et al. (*16*) reasoned if Ca^{2+} binding to the N-domain of TnC increases the solvent accessibility of hydrophobic residues, then replacement of these residues with more polar residues should increase the N-domain's Ca^{2+} affinity by reducing the energy required to drive the transition from the apo into the Ca^{2+} bound state. Therefore, Pearlstone et al. (*16*) studied Ca^{2+} binding to TnC^{F29W} and its mutants $V45TTnC^{F29W}$, $M46QTnC^{F29W}$, $M48ATnC^{F29W}$, $L49TTnC^{F29W}$ and $M82QTnC^{F29W}$. Indeed, these mutants exhibited increased Ca^{2+} affinities ranging from 1.8 μM for TnC^{F29W} to 691 nM for $M82QTnC^{F29W}$. These results were verified for M48ATnC and V45TTnC, which did not have the Phe → Trp mutation (*17*). There are other hydrophobic residues within the N-domain of TnC that undergo solvent accessibility changes upon Ca^{2+} binding (see Table 1). We examined whether the changes in the solvent exposure of these hydrophobic residues were the driving force determining how these residues influence Ca^{2+} binding to the N-domain of TnC or if other factors must also be considered.

The mutation Phe → Trp in position 29, immediately preceding the first Ca^{2+} binding loop, was previously used to study Ca^{2+} binding and exchange with the N-domain of TnC (*16*, *18*, *19*). We have utilized this mutation and introduced 27 additional mutations to examine the role of hydrophobic residues in Ca^{2+} binding and exchange with the N-terminal sites of TnC.

MATERIALS AND METHODS

Materials. Phenyl-Sepharose CL-4B and EGTA were purchased from Sigma Chemical Co. (St. Louis, MO). Quin-2 was purchased from Calbiochem (La Jolla, CA). All other chemicals were of analytical grade.

Protein Mutagenesis and Purification. Chicken skeletal TnC^{F29W} plasmid was a generous gift from Dr. Lawrence B. Smillie (University of Alberta, Edmonton, Alberta, Canada). TnC^{F29W} mutants were constructed from a TnC^{F29W} plasmid by primer-based site-directed mutagenesis using Stratagene's (La Jolla, CA) Quik-Change site-directed mutagenesis kit. The mutations were confirmed by DNA sequence analysis. The plasmids for TnC^{F29W} and mutants were transformed into *E. coli* BL21(DE3)pLysS cells (Novagen). Expression was induced by adding 0.4 mM IPTG when the bacterial cell density reached an OD_{600} of 0.6−0.8. After an additional 3 h of growth, cells were harvested and broken by sonication with a Branson Sonifier (Branson Ultrasonic Corporation, Danbury, CT). Cell debris were removed by centrifugation, and solid ammonium sulfate was added to the supernatant to 35% saturation. After centrifugation, the supernatant was purified by phenyl-Sepharose chromatography and DEAE Sepharose chromatography. We generally obtained 15−45 mg of purified protein from 1 L of bacterial culture. The purity of the proteins was checked by SDS−PAGE and determined to be 97 ± 5%, using a GS 300 transmittance/reflectance scanning densitometer (Hoefer Scientific Instru-

ments, San Francisco, CA). The purified TnC^{F29W} and mutants were dialyzed against three exchanges of 4 L of 10 mM MOPS, 90 mM KCl, pH 7.0 at 4 °C.

Determination of Ca^{2+} Affinities. All steady-state fluorescence measurements were performed using a Perkin-Elmer LS5 spectrofluorimeter at 15 °C. Trp fluorescence was excited at 275 nm and monitored at 345 nm as microliter amounts of $CaCl_2$ were added to 1 mL of each TnC^{F29W} mutant (0.3 μM) in 200 mM MOPS (to prevent pH changes upon addition of Ca^{2+}), 90 mM KCl, 2 mM EGTA, 1 mM DTT, pH 7.0, at 15 °C. The $[Ca^{2+}]_{free}$ was calculated using the computer program EGCA02 developed by Robertson and Potter (*20*). Ca^{2+} stock concentrations were measured using a Varian Techtron AA-575 atomic absorption spectrophotometer (Varian Instruments, Walnut Creek, CA).

The Ca^{2+} affinities were reported as a dissociation constant K_d, representing a mean of three to five titrations ± SD. Some of the mutants experienced an initial decrease in Trp fluorescence (up to 15% of the total fluorescence change), possibly associated with Ca^{2+} binding to the C-domain, followed by an increase in Trp fluorescence, associated with Ca^{2+} binding to the N-domain. K_d was calculated from the increases in Trp fluorescence for all of the mutants with the exception of $I37QTnC^{F29W}$. The data were fit with the logistic sigmoid function (mathematically equivalent to the Hill equation),

$$Y = Y_{min} + \frac{Y_{max} - Y_{min}}{1 + \exp[-k(X - X_{50})]}$$

where Y_{min} and Y_{max} represent the minimal and maximal Trp fluorescence, k is proportional to the Hill coefficient ($k = -n \ln 10$, where n is the Hill coefficient), X is the negative logarithm of $[Ca^{2+}]_{free}$, and X_{50} is the negative logarithm of $[Ca^{2+}]_{free}$ producing half-maximal fluorescence, as previously described (*14*).

Determination of Ca^{2+} Dissociation Rates. Ca^{2+} dissociation rates (k_{off}) were measured using an Applied Photophysics Ltd. (Leatherhead, U.K.) model SX.18 MV stopped-flow instrument with a dead time of 1.4 ms at 15 °C. The samples were excited using a 150 W xenon arc source. The Trp emission was monitored through a UV-transmitting black glass filter (UG1 from Oriel (Stanford, CT)). Each k_{off} represents an average of at least five traces, and the data were fit with a single exponential (variance less than 6.0×10^{-4}). The k_{off} was also measured using the fluorescent chelator Quin-2. Quin-2 was excited at 330 nm with its emission monitored through a 510 nm broad band-pass interference filter (Oriel (Stanford, CT)). Each k_{off} represents an average of at least five traces, and the data were fit with a double exponential (variance less than 1.3×10^{-4}) to account for the fact that Quin-2 reports the rates of Ca^{2+} dissociation from both N- and C-domains of TnC^{F29W}. The buffer used in all stopped-flow experiments was 10 mM MOPS, 90 mM KCl, 1 mM DTT, pH 7.0.

Determination of Ca^{2+} Association Rates. The Ca^{2+} association rates (k_{on}) were calculated using the relationship $k_{on} = k_{off}/K_d$, where k_{off} represents the concerted release of two Ca^{2+} ions and K_d represents the binding event of two Ca^{2+} ions to the N-domain of TnC, as previously described (*14*).

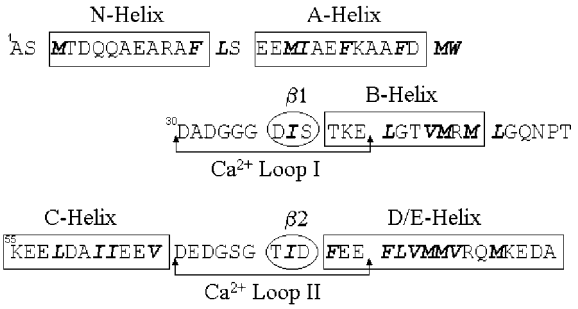

FIGURE 1: Amino acid sequence of the N-domain of TnC^{F29W}. Amino acid sequence of the first 90 residues of TnC^{F29W} is shown. Hydrophobic residues that were mutated are bold and italic, helices are boxed, arrows indicate loops, and β-sheet residues are circled.

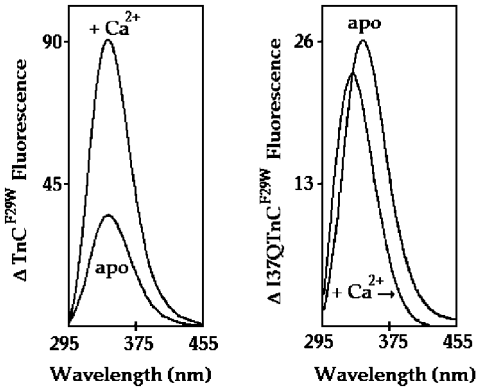

FIGURE 2: Effect of Ca^{2+} on the fluorescence spectra of TnC^{F29W} and $I37QTnC^{F29W}$. Fluorescence emission spectra for TnC^{F29W} (on the left) or $I37QTnC^{F29W}$ (on the right) are shown in the apo and Ca^{2+} bound states. The Trp fluorescence spectra were recorded with an excitation wavelength of 275 nm. The TnC^{F29W} and $I37QTnC^{F29W}$ concentration was 1 μM in 200 mM MOPS, 90 mM KCl, 2 mM EGTA, 1 m M DTT, pH 7.0, at 15 °C. TnC^{F29W} or $I37QTnC^{F29W}$ Trp fluorescence spectra were recorded before the addition of metal (apo) and after the addition of 1 mM free Ca^{2+} ($+Ca^{2+}$).

Calculation of Solvent Accessibilities. We have utilized the protein analysis software MOLMOL (*21*) to calculate the solvent-accessible surface areas for all N-terminal hydrophobic residues of chicken skeletal TnC. Apo and Ca^{2+} bound crystallographic and NMR structures of TnC are available from the Protein Data Bank (1TOP (*22*); 1NCZ and 1NCX (*23*); 4TNC (*24*); 1ZAC and 1SKT (*25*); 1AVS (*26*); 1TNX and 1TNW (*27*)). The solvent accessibility SA (in percent) for the mutated hydrophobic residue was then calculated as previously described (*28*) and was represented as a mean ± SD (Table 1).

RESULTS

Effect of Ca^{2+} on the Fluorescence Spectra of TnC^{F29W} and Mutants. TnC^{F29W} undergoes a large increase in Trp fluorescence upon Ca^{2+} binding to its N-terminal regulatory sites (*16*, *18*). To determine the role of hydrophobic residues in Ca^{2+} binding and exchange, we generated 27 TnC^{F29W} mutants in which we replaced individually all N-terminal hydrophobic Phe, Ile, Leu, Val, and Met residues with polar Gln (Figure 1). Addition of Ca^{2+} led to the changes in the fluorescence spectra of the mutant that were similar to that of TnC^{F29W} (data not shown) except for $I37QTnC^{F29W}$. Figure 2 shows fluorescence emission spectra of TnC^{F29W} (on the left) or $I37QTnC^{F29W}$ (on the right) in the absence and

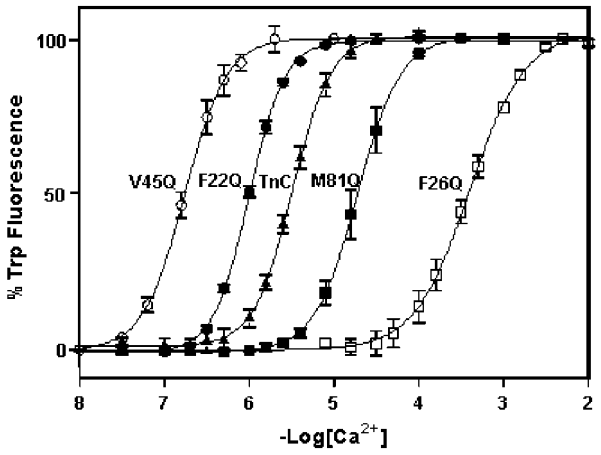

FIGURE 3: Ca^{2+} binding to TnC^{F29W} and its mutants. The Ca^{2+}-dependent increase in Trp fluorescence is shown as a function of $-\log [Ca^{2+}]$ for $V45QTnC^{F29W}$ (○, V45Q), $F22QTnC^{F29W}$ (●, F22Q), TnC^{F29W} (▲, TnC), $M81QTnC^{F29W}$ (■, M81Q), and $F26QTnC^{F29W}$ (□, F26Q). Microliter amounts of Ca^{2+} were added to 1 mL of each protein (0.3 μM) in 200 mM MOPS, 90 mM KCl, 2 mM EGTA, 1 mM DTT, pH 7.0, at 15 °C. The free $[Ca^{2+}]$ was calculated as described in Materials and Methods. Trp fluorescence emission was monitored at 345 nm with excitation at 275 nm. The data were normalized individually for each mutant, with the lowest value of Trp fluorescence set to 0% and with the highest value set to 100%. Each data point represents a mean ± SD of three to five titrations.

presence of Ca^{2+} at 15 °C. Upon Ca^{2+} binding, TnC^{F29W} underwent ~2.5-fold increase in its maximal Trp fluorescence at 345 nm. In contrast, $I37QTnC^{F29W}$ underwent ~1.3-fold decrease in its Trp Fluorescence at 345 nm and ~15 nm blue shift in maximal fluorescence intensity (from 345 nm in the apo state to 330 nm in the Ca^{2+} bound state). Analysis of crystal and NMR structures of TnC indicates that the side chain of Phe 29 comes in close contact with the side chain of Ile 37 in the apo and Ca^{2+} bound states (*22, 27*). Therefore, it is possible that the polar Gln in position 37 affects the local environment of Trp 29. On the other hand, there is a possibility that substitution of Ile 37 with Gln led to global conformational changes in the structure of TnC^{F29W}. Without additional structural data, we are currently unable to distinguish between the two possibilities.

Measurements of Ca^{2+} Binding Affinities for TnC^{F29W} and Mutants. Following the Ca^{2+}-induced changes in Trp fluorescence, we measured Ca^{2+} binding affinities (K_d) for each mutant at 15 °C. Examples of the Ca^{2+}-dependent increases in Trp fluorescence, which occur when Ca^{2+} binds to the N-terminal sites of TnC^{F29W}, $V45QTnC^{F29W}$, $F22QTnC^{F29W}$, $M81QTnC^{F29W}$ and $F26QTnC^{F29W}$, are shown in Figure 3. For the rest of the mutants, the results are summarized in Table 1. TnC^{F29W} exhibited a half-maximal Ca^{2+}-dependent increase in its Trp fluorescence at 3.2 μM. The Ca^{2+} affinities for the mutants ranged from 395 μM for $F26QTnC^{F29W}$ to 169 nM for $L49QTnC^{F29W}$. Therefore, substitution of hydrophobic residues with polar Gln produced N-domain TnC^{F29W} mutants exhibiting ~2340-fold variation in their Ca^{2+} affinities. Clearly, substitution of a single hydrophobic residue with polar Gln can produce a dramatic effect on Ca^{2+} binding to the N-domain of TnC^{F29W}.

The Hill coefficients for most of the mutants examined were between 1.2 and 2.3 (see Table 1) with the exception of $I37QTnC^{F29W}$, $L42QTnC^{F29W}$, and $I62QTnC^{F29W}$. For these three mutants, Hill coefficients were less than 1.2, indicating an absence of cooperativity between the first and second EF-hands (*29*). For $I37QTnC^{F29W}$ and $I62QTnC^{F29W}$, reduction in cooperativity appears to correlate with a dramatic decrease in Ca^{2+} affinity. These results indicate that for most of the hydrophobic residue substitutions, the cooperativity of interaction between the first and second EF-hands was not severely affected.

Relationship between the Ca^{2+} Affinity and Solvent Accessibility. Table 1 shows the SA (in percent) for the N-terminal hydrophobic residues in the apo state and in the Ca^{2+} bound state and the difference between the two states calculated from crystallographic and NMR structures of chicken TnC. When the values for all 27 mutants were used, there was no correlation between the Ca^{2+} affinity of the proteins with the SA of the mutated hydrophobic residues in the apo state (r^2 = 4%) and the Ca^{2+} bound state (r^2 = 6%) or with the difference between the two states (r^2 = 2%) (data not shown). This fact was also true if crystallographic and NMR structures were used independently (data not shown). Furthermore, the mutations that had little effect on the Ca^{2+} binding affinity (less than 2-fold higher or lower than that of TnC^{F29W}) on average experienced the same ~15% change (increase or decrease) in their SA as the mutations that dramatically (more than 2-fold) increased or decreased Ca^{2+} affinity. Thus, the SA change of the amino acid was a poor predictor of how its mutation affects Ca^{2+} affinity. However, the average of the apo state SA (~23%) for the hydrophobic amino acids that had little effect on the Ca^{2+} affinity upon mutation was ~6-fold higher than the average of the apo state SA (~4%) for the mutations that drastically increased or decreased Ca^{2+} affinity. Therefore, a majority of the mutations that had a large affect on Ca^{2+} affinity was almost completely buried in the apo state.

Measurements of Ca^{2+} Dissociation Rates Using Trp and Quin-2 Fluorescence. We conducted fluorescence stopped-flow measurements using EGTA-induced changes in Trp fluorescence to determine the rates of Ca^{2+} dissociation from the N-terminal sites of TnC^{F29W} and its mutants. Examples of the EGTA-induced decrease in Trp fluorescence at 15 °C are shown for $V45QTnC^{F29W}$, $F22QTnC^{F29W}$, TnC^{F29W}, $M81QTnC^{F29W}$, and $F26QTnC^{F29W}$ (Figure 4A). At 15 °C, EGTA removed Ca^{2+} from TnC^{F29W}at 340 s^{-1}. We were unable to determine the rate of Ca^{2+} dissociation from the lowest affinity mutant $F26QTnC^{F29W}$ because the reaction was complete during the mixing time of the instrument and was therefore too fast to observe. For the rest of the mutants, the Ca^{2+} dissociation rates ranged from 25 s^{-1} for $V45QTNC^{F29W}$ to 1137 s^{-1} for $I62QTnC^{F29W}$ (Table 1). Therefore, substitution of hydrophobic residues with polar Gln produced TnC^{F29W} mutants with more than 45-fold variation in their N-terminal Ca^{2+} dissociation rates.

The rates of Ca^{2+} dissociation were also measured using the fluorescent Ca^{2+} chelator Quin-2 (Figure 4B). The results show that for all of the mutants, except $I37QTnC^{F29W}$, the Ca^{2+} dissociation rate reported by Trp was in excellent agreement with the rate determined by Quin-2. Therefore, in all cases but one, Trp accurately reported the rate of Ca^{2+} dissociation from the N-terminal sites of TnC^{F29W}. Interestingly, for $I37QTnC^{F29W}$, the Ca^{2+} dissociation rate determined using Quin-2 was 1.8-fold slower than that reported by Trp. Therefore, for this mutant, it appears that the Trp fluorescence

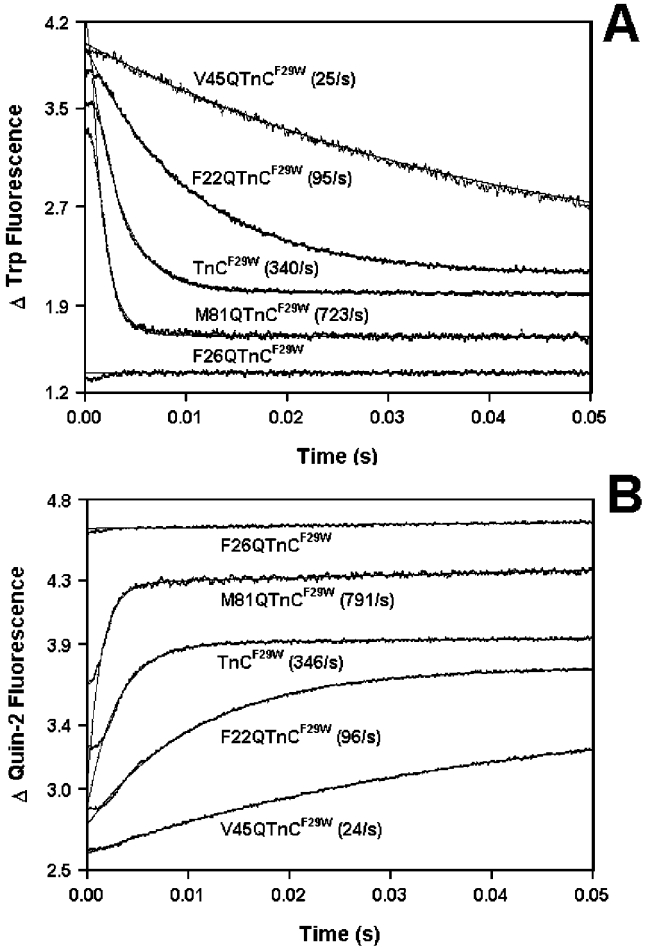

FIGURE 4: Rates of Ca^{2+} dissociation from TnC^{F29W} and its mutants. Panel A shows the time course of the decrease in Trp fluorescence as Ca^{2+} is removed by EGTA from V45QTnC^{F29W}, F22QTnC^{F29W}, TnC^{F29W}, M81QTnC^{F29W}, and F26QTnC^{F29W}. Each protein (1.2 μM) with 200 μM Ca^{2+} in 10 mM MOPS, 90 mM KCl, and 1 mM DTT, pH 7.0, was rapidly mixed with an equal volume of EGTA (5 mM) in the same buffer at 15 °C. Trp fluorescence was monitored through a UV-transmitting black glass filter (UG1 from Oriel, Stanford, CT) with excitation at 275 nm. All kinetics traces were triggered at time zero, and the first 1.4 ms of premixing is shown. The traces were fit after mixing was complete, as described in Materials and Methods. The traces have been normalized and displaced vertically for clarity. Panel B shows the time course of the increase in Quin-2 fluorescence as Ca^{2+} is removed by Quin-2 from the N-terminal sites of V45QTnC^{F29W}, F22QTnC^{F29W}, TnC^{F29W}, M81QTnC^{F29W}, and F26QTnC^{F29W}. Each protein (6 μM) with 60 μM Ca^{2+} in the same buffer as in panel A was rapidly mixed with an equal volume of Quin-2 (150 μM) in the same buffer at 15 °C. Quin-2 fluorescence was monitored through a 510 nm broad band-pass interference filter with excitation at 330 nm. The traces have been normalized and displaced vertically for clarity.

reports a faster conformational change rather than the true rate of Ca^{2+} dissociation. After the data for all of the mutants were analyzed, there was no strong correlation between Ca^{2+} affinities and Ca^{2+} dissociation rates ($r^2 = 0.28$, data not shown); therefore, for at least some of the mutants the Ca^{2+}-association rate must change.

Calculation of Ca^{2+} Association Rates. After measuring the Ca^{2+} dissociation constants (K_d) and the Ca^{2+} dissociation rates (k_{off}, using the Trp fluorescence), we calculated the Ca^{2+} association rates ($k_{on} = k_{off}/K_d$) for TnC^{F29W} and its mutants. We previously demonstrated that the calculated k_{on} for TnC^{F29W} is in excellent agreement with the experimentally measured k_{on} (*18*). TnC^{F29W} mutants exhibited less than 70-fold variation in their Ca^{2+} association rates, ranging from faster than 0.03×10^8 M^{-1} s^{-1} for F26QTnC^{F29W} to 2.1×10^8 M^{-1} s^{-1} for L49QTnC^{F29W}. Table 1 compares Ca^{2+} affinities (K_d), Hill coefficients, Ca^{2+} dissociation rates (k_{off}) measured using Trp and Quin-2 fluorescence, Ca^{2+} association rates (k_{on}), solvent accessibility (SA) in apo and Ca^{2+} bound states, and the difference in SA between Ca^{2+} bound and apo states for TnC^{F29W} and its mutants. Clearly, while some of the mutations alter Ca^{2+} affinity without significantly changing the rate of Ca^{2+} association, others affect both Ca^{2+} association and dissociation rates.

DISCUSSION

The mechanisms that determine the vast range of Ca^{2+} affinities and exchange rates in EF-hand Ca^{2+} binding proteins have been elusive. It is clear that the chelating residues, especially in the $+x$ and $-z$ positions, are important for Ca^{2+} binding to EF-hand proteins (for review, see refs *30*−*32*). However, the character of the chelating residues alone cannot account for the wide variety of Ca^{2+} affinities and exchange rates (for review, see refs *10*, *11*, *13*, *14*). The goal of this study was to examine the role of hydrophobic residues in Ca^{2+} binding and exchange with the N-domain of TnC. Since chicken skeletal TnC has no intrinsic fluorescent probes, we utilized the fluorescence of TnC^{F29W}, which has been previously used to study Ca^{2+} and ligand binding to the N-terminal sites of TnC and its mutants (*16*, *18*, *32*−*37*). Since all of the mutants exhibited Ca^{2+}-dependent changes in their Trp fluorescence spectra, we were able to compare Ca^{2+} binding affinities of the mutants to that of TnC^{F29W}. The half-maximal Ca^{2+} binding to TnC^{F29W} occurred at 3.2 μM at 15 °C. This value is in good agreement with the Ca^{2+} affinity reported for TnC^{F29W} at 20 °C (*16*). The mutants exhibited ~2340-fold variation in their Ca^{2+} affinities, ranging from 169 nm for L49QTnC^{F29W} to 395 μM for F26QTnC^{F29W}.

Clearly, mutation of hydrophobic residues to polar Gln in the N-domain of TnC^{F29W} can both dramatically increase and decrease Ca^{2+} affinity (Table 1). There was no consistent pattern in how a single type of hydrophobic residue modified Ca^{2+} affinity. For instance, mutation of Val 45 increased Ca^{2+}affinity 18.8-fold, whereas mutation of Val 80 decreased Ca^{2+}affinity 6.9-fold and mutation of Val 83 had little effect on the Ca^{2+} affinity. Furthermore, there was no correlation between the Ca^{2+} affinity of the 27 mutant proteins and the solvent accessibility of the mutated hydrophobic residues in either the absence or presence of Ca^{2+} (or the difference between the two states). Thus, the change in solvent exposure of a hydrophobic residue is not the sole determinant in how the residue affects Ca^{2+} binding.

We propose that the side chain interactions of the hydrophobic residues within the tertiary structure of the apo and Ca^{2+} bound N-domain of TnC play a dominant role in dictating Ca^{2+}affinity. To evaluate this hypothesis, we have separated the hydrophobic residues into three main groups based on the effect of their mutations on the N-domain Ca^{2+} binding affinities: (1) hydrophobic residue mutations that increase Ca^{2+} affinity more than 2-fold; (2) hydrophobic residue mutations that decrease Ca^{2+}affinity more than 2-fold, and (3) hydrophobic residue mutations that had little to no

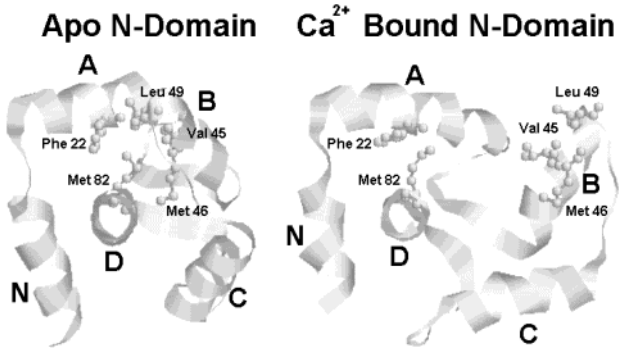

FIGURE 5: Hydrophobic residue mutations that increase Ca^{2+} affinity. The crystal structure of the apo N-domain of TnC is shown on the left (PDB file 1TOP (*22*)). The NMR structure of the Ca^{2+} bound N-domain of TnC is shown on the right (PDB file 1TNX (*27*)). This figure was drawn using Rasmol (*49*). Helices are labeled (N, A, B, C, and D) and shown as ribbons; hydrophobic residue mutations that increase Ca^{2+} affinity more than 2-fold (Phe 22, Val 45, Met 46, Leu 49, and Met 82) are shown in a ball-and-stick format and are labeled.

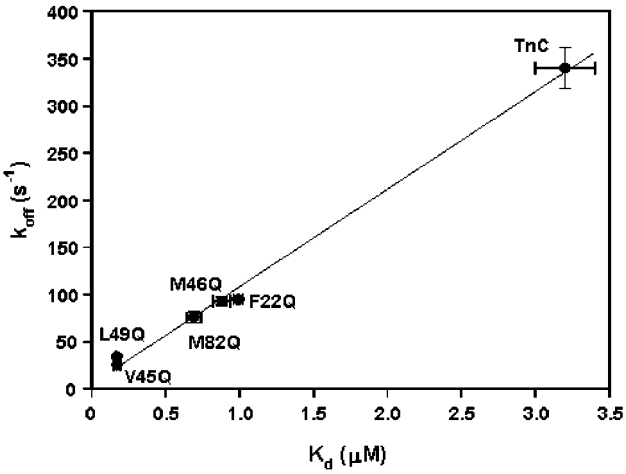

FIGURE 6: Correlation between Ca^{2+} affinity (K_d) and dissociation rate (k_{off}) for $F22QTnC^{F29W}$ (F22Q), $V45QTnC^{F29W}$ (V45Q), $M46QTnC^{F29W}$ (M46Q), $L49QTnC^{F29W}$ (L49Q), $M82QTnC^{F29W}$ (M82Q), and TnC^{F29W} (TnC). The solid line was obtained by fitting the data with a linear regression. Each data point represents a mean ± SD of three to five separate experiments. The correlation coefficient (r^2) is 0.99.

effect on the Ca^{2+}affinity compared to TnC^{F29W}. The proposed molecular mechanisms for each group are discussed below.

Hydrophobic Residue Mutations That Increase Ca^{2+} Affinity. We propose that residues Phe 22, Val 45, Met 46, Leu 49, and Met 82 act as apo interunit stabilizers. Substitution of these hydrophobic residues with polar Gln led to large (more than 2.0-fold) increases in Ca^{2+} affinity of the N-domain. As previously mentioned, when Ca^{2+} binds to the N-terminal EF-hands of TnC, the BC unit moves away from the NAD unit to open the hydrophobic pocket. Earlier studies suggest that mutations that stabilize the BC and NAD units' interactions in the apo state, through disulfide bond or salt bridge formation, decrease the Ca^{2+} affinity of the regulatory domain (*38*, *39*). On the other hand, mutations that shift the equilibrium of TnC toward the Ca^{2+} bound state, by reducing the amount of hydrophobic exposure in the presence of Ca^{2+}, increase the Ca^{2+} affinity of the regulatory domain (*16*). Thus, one determinant of the Ca^{2+}affinity is the amount of energy required to open the hydrophobic pocket through the movement of the BC unit relative to the NAD unit.

Val 45, Met 46, and Leu 49 are located as a cluster within the BC unit, whereas Phe 22 and Met 82 are located as a cluster within the NAD unit (Figure 5). In the apo state of the N-domain, these two clusters of hydrophobic residues form extensive side chain interactions. Upon Ca^{2+} binding to the N-domain of TnC, these two hydrophobic clusters move away from one another as the BC unit moves away from the NAD unit. Therefore, substitution of these hydrophobic residues with polar Gln should reduce the hydrophobic contacts between the BC and NAD units in the apo state (destabilize the apo state) and shift the equilibrium toward the Ca^{2+} bound state. In addition, upon binding Ca^{2+} , these hydrophobic residues increase their solvent accessibility. Thus, substitution of these hydrophobic residues with polar Gln allows easier opening of the hydrophobic pocket by reducing the energy needed to drive the transition from the apo into Ca^{2+} bound state. Furthermore, these TnC^{F29W} mutants were the only group that exhibited a strong correlation between the rate of Ca^{2+} dissociation and Ca^{2+} affinity ($r^2 = 0.99$, Figure 6). Therefore, increases in Ca^{2+} affinity observed with these mutants were largely due to the decreases in Ca^{2+} dissociation rate, further supporting the idea that the Ca^{2+} bound state is preferentially stabilized.

Met 36 and Met 72 of the closely related Ca^{2+} binding protein, CaM, correspond to Met 46 and Met 82 of TnC. In the apo state of CaM (*40*), the side chains of Met 36 and Met 72 interact, whereas in the Ca^{2+} bound state (*41*) they move away from one another. Substitution of either one of these two residues, or both, with Gln increased the Ca^{2+}-affinity and decreased the Ca^{2+} dissociation rate from the N-domain of CaM (*42*). Furthermore, when Met 36 or Met 72 was mutated to the more hydrophobic Leu residue, the Ca^{2+}affinity of the N-domain was decreased while the Ca^{2+} dissociation rate was increased (*42*). Thus, it appears that some of the mechanisms that control the Ca^{2+}-dependent opening of the hydrophobic pocket in TnC are similar for CaM and possibly for other Ca^{2+}binding proteins.

Hydrophobic Residue Mutations That Decrease Ca^{2+} Affinity. Substitution of Phe 26, Ile 37, Ile 62,Val 65, Ile 73, Phe 78, Leu 79, Val 80, or Met 81 with polar Gln led to large (more than 2.0-fold) decreases in Ca^{2+} affinity of the N-domain. In both the apo and Ca^{2+} bound states, these residues are clustered at the center of the hydrophobic pocket, surrounding the two Ca^{2+} binding loops. Among these residues, only Ile 62 underwent a decrease in solvent accessibility upon Ca^{2+} binding to the N-domain of TnC. Therefore, as previously pointed out, the change in solvent accessibility of a hydrophobic residue is not the main factor that determines the role of this residue in Ca^{2+} binding. In addition, no correlation between Ca^{2+} affinity and Ca^{2+} dissociation rate was observed for these mutants ($r^2 = 0.26$, data not shown). In fact, the dramatic decreases in Ca^{2+} affinity observed in these mutants were in part due to the large decreases in the rates of Ca^{2+} association (Table 1). The results for this group differ from those obtained for mutants of calbindin D_{9k}, where substitution of hydrophobic residues with Ala and Gly in the center of the hydrophobic core decreased Ca^{2+} affinity mainly through increases in Ca^{2+} dissociation rate (*15*). We have further divided these

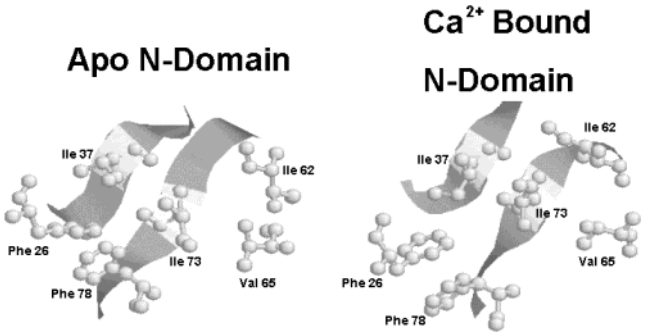

FIGURE 7: β-Sheet hydrophobic residues and β-sheet interacting residues. The β-sheet hydrophobic residues (Ile 37 and Ile 73) and β-sheet interacting residues (Ile 26, Ile 62, Val 65, and Phe 78) within apo (on the left) and Ca^{2+} bound N-domain of TnC (on the right) are shown in a ball-and-stick format and are labeled. The PDB files used in this figure are the same as in Figure 5.

hydrophobic residues into four, sometimes overlapping, subgroups: β-sheet residues, β-sheet interacting residues, a hinge residue, and D-helix residues.

β-Sheet Residues. Ile 37 and Ile 73 (β-sheet residues) are in the middle of the three-residue β-strands, located in the first and second Ca^{2+} binding loops, which interact to form an antiparallel β-sheet (Figure 7). The residues located in the middle of the β-sheets in various EF-hand proteins are almost exclusively hydrophobic. Individual mutations of these hydrophobic β-sheet residues to either more polar or smaller hydrophobic residues in two other EF-hand proteins, calmodulin and calbindin D_{9k}, led to decreased Ca^{2+} affinity and in some cases decreased cooperativity of Ca^{2+} binding (*15*, *43*). In TnC^{F29W}, substitution of Ile 37 and Ile 73 with polar Gln led to 24- and 7-fold reductions in Ca^{2+} affinity, respectively. The Ca^{2+} dissociation rates are only slightly increased by these mutations, while Ca^{2+} association rates are dramatically slowed. These results differ from those obtained for CaM, where substitution of C-domain β-sheet hydrophobic residues with Gly reduced Ca^{2+} affinity through a large increase in the Ca^{2+} dissociation rate combined with a smaller increase in the Ca^{2+} association rate (*43*). It is possible that hydrophobic β-sheet mutations interfere with the ability of TnC to bind Ca^{2+} by perturbing the structure of the Ca^{2+} binding loops.

β-Sheet Interacting Residues. Residues Phe 26, Ile 62, Val 65, and Phe 78 form another subgroup, the β-sheet interacting residues. Phe 26 and Ile 62 precede the first and second Ca^{2+} binding loops by four amino acids, respectively. Analysis of 3232 EF-hand sequences (obtained from the Sanger Center's protein families database of alignments and HMMs (PFaM) at http://www.cgr.ki.se/cgi-bin/Pfam/getacc?PF00036) determined that the residue that precedes the Ca^{2+} binding loop by four amino acids is 97% hydrophobic and is occupied by Phe and Ile in 56% and 17% of these sequences, respectively. Analysis of crystal and NMR structures of TnC indicates that Phe 26 makes extensive side chain contacts with Ile 37 in both the apo and Ca^{2+} bound states of the N-domain, whereas the side chain of Ile 62 closely interacts with the side chain of Ile 73 only in the Ca^{2+}bound state (Figure 7). Substitution of Phe 26 and Ile 62 with Gln led to 123- and 12-fold decreases in Ca^{2+} affinity of the N-domain, respectively. Both of these mutations decrease Ca^{2+} affinity through the slowing of Ca^{2+} association rates and speeding of Ca^{2+} dissociation rates. Our studies show that these conserved hydrophobic residues are even more crucial for maintaining high Ca^{2+} binding affinity and cooperativity than the conserved β-sheet hydrophobic residues.

Similarly, in the apo state, the hydrophobic side chains of Val 65 and Phe 78 are in close contact with the side chain of Ile 73, while the side chain of Val 65 also interacts with the side chain of Ile 62. Furthermore, Phe 78 makes extensive side chain interactions with Phe 26 in the absence and presence of Ca^{2+} (Figure 7). Thus, one potential role for Val 65 and Phe 78 is to stabilize the β-sheet aiding in the preformation of the Ca^{2+} binding loops. Similarly, in calbindin D_{9K}, substitution of Phe 10 and Leu 28, which have side chain interactions with the conserved hydrophobic β-sheet residues in both apo and Ca^{2+} bound states with smaller and less hydrophobic residues, decreased the global Ca^{2+} affinity of the protein (*15*). Thus, to maintain high Ca^{2+} affinity in a paired EF-hand system, it is important to stabilize the β-sheets in both the absence and the presence of Ca^{2+}.

Interestingly, carbonic anhydrase II partially coordinates zinc binding through two His residues located on a β-strand. These two His residues are flanked by three hydrophobic residues that pack with a conserved aromatic cluster beneath the zinc binding site (*44*). Reducing the hydrophobic character by mutation of the hydrophobic β-strand residues distorted the zinc ligating geometry and decreased zinc affinity (*45*, *46*). Thus, it is possible that in TnC, like in carbonic anhydrase II, some of the hydrophobic residues are utilized to maintain the proper cation coordination geometries.

Hinge Residue. The movement of the BC unit relative to the NAD unit is accompanied by large changes in the dihedral angles of Val 65, which is thought to act as a hinge for the opening of the hydrophobic pocket (*25*). Substitution of Val 65 with Gln led to a 2.5-fold decrease in Ca^{2+} affinity of the N-domain. This decrease in affinity was caused by a 2.8-fold slower Ca^{2+} association rate. Thus, it appears that mutation of the hinge residue impedes the opening of the hydrophobic pocket, possibly restricting the dihedral angle changes necessary for the reorientation of the BC unit. As mentioned before, in addition to being the hinge residue, Val 65 could possibly act as a β-sheet stabilizer.

D-Helix Residues. Residues Phe 78, Leu 79, Val 80, and Met 81 reside within the stretch of six consecutive hydrophobic amino acids (Phe 78 to Val 83) on the D-helix. One potential role for Phe 78 as a β-sheet stabilizer was discussed above. However, Phe 78, Leu 79, Val 80, and Met 81 extensively interact with different regions of the N and A helices in both the apo and Ca^{2+} bound states (Figure 8). While all four mutants exhibit slower Ca^{2+} association rates, $V80QTnC^{F29W}$ and $M81QTnC^{F29W}$ also exhibit faster Ca^{2+} dissociation rates. These residues may help to maintain the integrity of the NAD unit in both the apo and Ca^{2+} bound states. However, Met 81 comes in close contact with Glu 64 located in the C-helix. Therefore, an alternative explanation for the decrease in Ca^{2+}affinity observed with Met 81 → Gln mutation is that the Gln residue could potentially hydrogen-bond with the side chain of Glu 64 in the BC unit, making it more difficult to open the hydrophobic pocket. We are currently planning additional experiments designed to test this and other hypotheses put forward in this paper.

Hydrophobic Residue Mutations That Had Little or No Effect on Ca^{2+} Affinity. Substitutions of residues Met 3, Phe

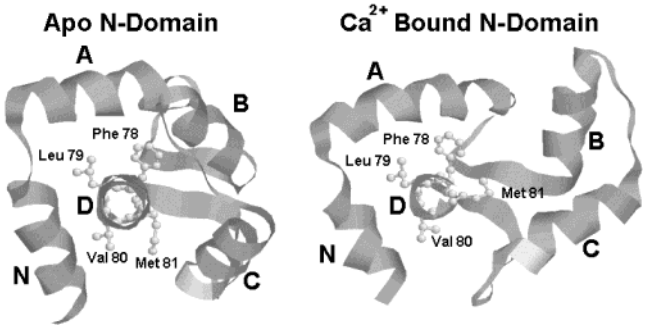

FIGURE 8: D-helix hydrophobic residues. Helices are labeled (N, A, B, C, and D) and are shown as ribbons. D-helix hydrophobic residues (Phe 78, Leu 79, Val 80, and Met 81) within the apo (on the left) or Ca^{2+} bound N-domain of TnC (on the right) are shown in a ball-and-stick format and are labeled. The PDB files used in this figure are the same as in Figure 5.

13, Met 18, Met 48, Ile 61, or Met 86 with Gln led to small (less than 2.0-fold) increases in Ca^{2+} affinity, while substitution of residues Leu 14, Ile 19, Met 28, Leu 42, Leu 58, Phe 75, or Val 83 with Gln led to small (less than 2.0-fold) reductions in Ca^{2+} affinity. Therefore, ~50% of the mutations had little or no effect on the Ca^{2+} binding properties of the N-domain of TnC^{F29W}. In the apo and Ca^{2+} bound states, these residues are scattered primarily around the exterior of the N-domain. Furthermore, these mutations did not lead to large alterations in Ca^{2+} association or dissociation rates, with the exception of $L42QTnC^{F29W}$ and $L58QTnC^{F29W}$. $L42QTnC^{F29W}$ exhibited a 2.8-fold slower Ca^{2+} association rate, while $L58QTnC^{F29W}$ exhibited a 2.0-fold faster Ca^{2+} dissociation rate, relative to TnC^{F29W}. In the Ca^{2+} bound state, the side chain of Leu 42 interacts with the side chains of Leu 58, Ile 37, Ile 62, and Ile 73 so that Leu 42 and Leu 58 could be involved in the stabilization of the β-sheet region. Interestingly, most of the residues with little to no affect on Ca^{2+} affinity were significantly exposed to solvent in the apo state. In fact, the average of the apo state SA (23%) for these hydrophobic residues was ~6-fold higher than the average of the apo state SA (4%) for the hydrophobic residues that drastically increase or decrease Ca^{2+} affinity upon mutation. One possible interpretation is that residues with significant exposure to solvent in the apo state possess fewer hydrophobic side chain interactions lost upon substitution with Gln and thus do not exert a large influence on the Ca^{2+} binding properties of the protein. In the end, it appears that the side chain interactions within the tertiary structure of the protein were critical in determining the role of the hydrophobic residue in Ca^{2+} binding and exchange.

The question of cooperativity of Ca^{2+} binding between the first and second EF-hands of TnC and TnC^{F29W} is controversial. Some evidence suggests that the first and second EF-hands bind Ca^{2+} in a cooperative manner (*16*, *47*), while other data suggest stepwise Ca^{2+} binding to the isolated N-domain of TnC (*32*, *34*). In the present work, titration curves for TnC^{F29W} and most of its mutants exhibited Hill coefficients higher than 1.2, suggesting cooperativity of Ca^{2+} binding between the first and second EF-hands of TnC^{F29W} (*29*). For $I37QTnC^{F29W}$, $L42QTnC^{F29W}$, and $I62QTnC^{F29W}$, Hill coefficients were less than 1.2, indicating an absence of Ca^{2+} binding cooperativity (*29*). As previously mentioned, it is possible that Ile 37, Leu 42, and Ile 62 stabilize the β-sheet region, making the loop configuration optimal for binding Ca^{2+}. However, Hill coefficients obtained from Ca^{2+} titration curves, as was done in this study, might not be a reliable measure of cooperativity (*32*). In addition, we cannot rule out the possibility that the Phe → Trp mutation by itself altered cooperativity between the first and second EF-hands of TnC. Nevertheless, our data seem to suggest that Ca^{2+} binding to the N-domain of TnC^{F29W} is cooperative, and this cooperativity is maintained via the β-sheet region. In fact, as Ca^{2+} binds to the N-domain of TnC, the β-sheet becomes less extended and less twisted, allowing Ca^{2+} binding to one EF-hand to be sensed by the other EF-hand (*26*, *48*).

In summary, we utilized Phe → Trp mutation in position 29 to study Ca^{2+} binding and exchange with the N-domain of TnC. We then made 27 TnC^{F29W} mutants in which we individually substituted all N-terminal hydrophobic Phe, Ile, Leu, Val, and Met with polar Gln. The TnC^{F29W} mutants exhibited ~2340-fold variation in their Ca^{2+} binding affinities, less than 70-fold variation in their Ca^{2+} association rates, and more than 45-fold variation in their Ca^{2+} dissociation rates. However, not all of the mutations had a dramatic effect on Ca^{2+} binding and exchange. Our results suggest that the side chain interactions of the hydrophobic residue within the tertiary structure of TnC were crucial in determining how the residue affects Ca^{2+} binding properties of the protein. These findings enhance understanding of the relationship between the structure and Ca^{2+} binding properties of TnC and possibly other EF-hand proteins.

ACKNOWLEDGMENT

We thank Dr. Lawrence B. Smillie for the generous gift of TnC^{F29W} plasmid and critical reading of the manuscript, Dr. Ruth A. Altschuld for critical reading of the manuscript, and Dr. Richard P. Swenson and Dr. Charles E. Bell for helpful discussion of the data.

REFERENCES

1. Farah, C. S., and Reinach, F. C. (1995) *FASEB J. 9*, 755−767.
2. Squire, J. M., and Morris, E. P. (1998) *FASEB J. 12*, 761−771.
3. Gordon, A. M., Homsher, E., and Regnier, M. (2000) *Physiol. Rev. 80*, 853−924.
4. Nelson, M. R., and Chazin, W. J. (1998) *Biometals 11*, 297−318.
5. Filatov, V. L., Katrukha, A. G., Bulargina, T. V., and Gusev, N. B. (1999) *Biochemistry (Moscow) 64*, 969−985.
6. Potter, J. D., and Gergely, J. (1975) *J. Biol. Chem. 250*, 4682−4633.
7. Sekharudu, Y. C., and Sundaralingam, M. (1988) *Protein Eng. 2*, 139−146.
8. Strynadka, N. C., and James, M. N. (1989) *Annu. Rev. Biochem. 58*, 951−998.
9. Marsden, B. J., Shaw, G. S., and Sykes, B. D. (1990) *Biochem. Cell. Biol. 68*, 587−601.
10. Falke, J. J., Drake, S. K., Hazard., A. L., and Peersen, O. B. (1994) *Q. Rev. Biophys. 27*, 219−290.
11. Linse, S., and Forsen, S. (1995) *Adv. Second Messenger Phosphoprotein Res. 30*, 89−151.
12. George, S. E., Su, Z., Fan, D., Wang, S., and Johnson, J. D. (1996) *Biochemistry 35*, 8307−8313.
13. Wang, S., George, S. E., Davis, J. P., and Johnson, J. D. (1998) *Biochemistry 37*, 14539−14544.
14. Black, D. J., Tikunova, S. B., Johnson, J. D., and Davis, J. P. (2000) *Biochemistry 39*, 13831−13837.

15. Kragelund, B. B., Jonsson, M., Bifulco, G., Chazin, W. J., Nilsson, H., Finn, B. E., and Linse, S. (1998) *Biochemistry 37*, 8926−8937.
16. Pearlstone, J. R., Borgford, T., Chandra, M., Oikawa, K., Kay, C. M., Herzberg, O., Moult, J., Herklotz, A., Reinach, F. C., and Smillie, L. B. (1992) *Biochemistry 31*, 6545−6553.
17. da Silva, A. C., de Araujo, A. H., Herzberg, O., Moult, J., Sorenson, M., and Reinach, F. C. (1993) *Eur. J. Biochem. 213*, 599−604.
18. Johnson, J. D., Nakkula, R. J., Vasulka, C., and Smillie, L. B. (1994) *J. Biol. Chem. 269*, 8919−8923.
19. Li, M. X., Chandra, M., Pearlstone, J. R., Racher, K. I., Trigo-Gonzalez, G., Borgford, T., Kay, C. M, and Smillie, L. B. (1994) *Biochemistry 33*, 917−925.
20. Robertson, S., and Potter, J. D. (1984) *Methods Pharmacol. 5*, 63−75.
21. Koradi, R., Billeter, M., and Wüthrich, K. (1996) *J. Mol. Graphics 14*, 51−55.
22. Satyshur, K. A., Pyzalska, D., Greaser, M., Rao, S. T., and Sundaralingam, M. (1994) *Acta Crystallogr., Sect. D: Biol. Crystallogr. 50*, 40−49.
23. Rao, S. T., Satyshur, K. A., Greaser, M. L., and Sundaralingam, M. (1996) *Acta Crystallogr., Sect. D: Biol. Crystallogr. 52*, 916−922.
24. Satyshur, K. A., Rao, S. T., Pyzalska, D., Drendel, W., Greaser, M., and Sundaralingam, M. (1988). *J. Biol. Chem. 263*, 1628−1647.
25. Tsuda, S., Miura, A., Gagne, S. M., Spyracopoulos, L., and Sykes, B. D. (1999) *Biochemistry 38*, 5693−5700.
26. Strynadka, N. C., Cherney, M., Sielecki, A. R., Li, M. X., Smillie, L. B., and James, M. N. (1997) *J. Mol. Biol. 273*, 238−255.
27. Slupsky, C. M., and Sykes, B. D. (1995) *Biochemistry 34*, 15953−15964.
28. Gromiha, M. M., Oobatake, M., Kono, H., Uedaira, H., and Sarai, A. (1999) *Protein Eng. 12*, 549−555.
29. Grabarek, Z., Grabarek, J., Leavis, P. C., and Gergely, J. (1983). *J. Biol. Chem. 258*, 14098−14102.
30. Babu, A., Su, H., and Gulati, J. (1993) *Adv. Exp. Med. Biol. 332*, 125−131.
31. Gagne, S. M., Li, M. X., and Sykes, B. D. (1997) *Biochemistry 36*, 4386-4392.
32. Pearlstone, J. R., Chandra, M., Sorenson, M. M., and Smillie, L. B. (2000) *J. Biol. Chem. 275*, 35106−35115.
33. Chandra, M., da Silva, E. F., Sorenson, M. M., Ferro, J. A., Pearlstone, J. R., Nash, B. E., Borgford, T., Kay, C. M., and Smillie, L. B. (1994) *J. Biol. Chem. 269*, 14988−14994.
34. Li, M. X., Gagne, S. M., Tsuda, S., Kay, C. M, Smillie, L. B., and Sykes, B. D. (1995) *Biochemistry 34*, 8330−8340.
35. Pearlstone, J. R., and Smillie, L. B. (1995) *Biochemistry 34*, 6932−6940.
36. Pearlstone, J. R., Sykes, B. D., and Smillie, L. B. (1997) *Biochemistry 36*, 7601−7606.
37. Leblanc, L., Bennet, A., and Borgford, T. (2000) *Arch. Biochem. Biophys. 384*, 296−304.
38. Fujimori, K., Sorenson, M., Herzberg, O., Moult, J., and Reinach, F. C. (1990) *Nature 345*, 182−184.
39. Grabarek, Z., Tan, R. Y., Wang, J., Tao, T., and Gergely, J. (1990) *Nature 345*, 132−135.
40. Kuboniwa, H., Tjandra, N., Grzesiek, S., Ren, H., Klee, C. B., and Bax, A. (1995) *Nat. Struct. Biol. 2*, 768−776.
41. Chattopadhyaya, R., Meador, W.E., Means, A. R., and Quiocho, F. A. (1992) *J. Mol. Biol. 228*, 1177−1192.
42. Black, D. J. (2001) *Biophys. J. 80*, 408a.
43. Browne, J. P., Strom, M., Martin, S. R., and Bayley, P. M. (1997) *Biochemistry 36*, 9550−9561.
44. Hakansson, K., Carlsson, M., Svensson, L. A., and Liljas, A. (1992) *J. Mol. Biol. 227*, 1192−1204.
45. Hunt, J. A., and Fierke, C. A. (1997) *J. Biol. Chem. 272*, 20364−20372.
46. Hunt, J. A., Ahmed, M., and Fierke, C. A. (1999) *Biochemistry 38*, 9054−9062.
47. Golosinska, K., Pearlstone, J. R., Borgford, T., Oikawa, K., Kay, C. M., Carpenter, M. R., and Smillie, L. B. (1991) *J. Biol. Chem. 266*, 15797−15809.
48. Houdusse, A., Love, M. L., Dominguez, R., Grabarek, Z., and Cohen, C. (1997) *Structure 5*, 1695−1711.
49. Sayle, R. A., and Milner-White, E. J. (1995) *Trends Biochem. Sci. 20*, 374−376.

BI011763H